Performance of a Novel Planar-Processed Avalanche Photodiode for Light and x-ray Detection

Ernesto Gramsch[a,*] and Ricardo E. Avila[b]

[a]Departamento de Física, Universidad de Santiago, Avda. Ecuador 3493, Santiago, Chile

[b]Departamento de Materiales Nucleares, Comisión Chilena de Energía Nuclear, Casilla 188-D, Santiago, Chile

Abstract

We have performed a detailed investigation of the light and x-ray response of a newly developed planar avalanche photodiode (APD) of the deep diffused type. This type of photodetector design has the low noise characteristics obtained from the deep diffusion process, but it is built using only standard planar technology. We measured an excess noise factor of 1.8 at a gain of 6, which is similar to other commercial APDs. With this type of structure, the expected gain is ~ 500 at 1600 V. We have not achieved this gain because there is early breakdown at the surface. Future designs will incorporate improvements in the structure to avoid surface breakdown. In spite of this, the low noise obtained at a gain of 6, indicates that this structure, reaching full breakdown, has potential to work with very low noise. At this gain, it is found that the dominant contribution to the broadening of the energy resolution comes from preamplifier voltage noise. The measured capacitance was 20 pF, and the rise time 11 ns at 1300 V. The dependence of the gain with the density of generated carriers has also been investigated. When the gain is measured with α

---

[*] Corresponding author, Tel: (56-2) 776 33 22, Fax: (56-2) 776 95 96, e-mail:egramsch@lauca.usach.cl

particles (large number of electrons injected into an area of a few μm), it is lower than the gain measured with light. The decrease starts to be seen at a gain of 2. When a large amount of charge (90 x 10^6 e) is injected via a light pulse into a larger area (0.3 mm diameter), no effect is seen.

Subject terms: avalanche photodiode; planar design; low noise detector; deep diffusion

I. Introduction

The trend in many systems that use semiconductor detectors goes towards obtaining higher output with fast response time. A variety of new optical techniques for biomedical, environmental, industrial, telecommunications, and other applications has stimulated the development of sensors that can meet stringent requirements. Most optical instruments in any field require detectors with a particular geometry, spectral response, speed or gain. An advantage of semiconductor detectors such as PIN and PN diodes, CCDs, phototransistors, etc. is that they can be easily redesigned for a particular instrument, and the time it takes to obtain a special geometry

is only a few months. This flexibility and short design time is probably the reason for its widespread use. Most semiconductor detectors are compact, rugged and have low power consumption, but they have no gain and rely on low noise preamplifiers to function adequately. They are used in lidar systems for atmospheric pollution measurements, positron emission tomography[1], photoluminescence[2], optical guidance, and so on. When it comes to high sensitivity, photomultiplier tubes are used most of the time. Because of the high gain, they are used for low light level, photon counting, timing applications, spectroscopy, medical imaging. However, it is not easy to redesign a PMT to fit a particular instrument. An intermediate solution for applications where high speed or high sensitivity is needed, are avalanche photodiodes. These detectors can be easily adapted to optical instruments that need different geometry, spectral response or gain.[3]

In this paper we will analyze in more detail the light and x-ray response a new avalanche photodiode of the deep diffused type[4]. In section II we will briefly describe the structure of the APD. In section III we will discuss the sources of electronic noise in the detector as well as the amplifier and compare the results with experimental data. In section IV we will look at the variation of the gain when large number of carriers are injected.

II. Detector Characteristics

The APD has been developed using only planar technology, that is, the reduction of the electric field at the edges is achieved using diffused rings [4]. The detector has the deep diffusion structure of traditional high gain APDs [5, 6], but it requires no beveling or etching that increases production costs. The approach used to reduce the electric field at the edges was to diffuse a multiple ring structure around the main junction. The front p-structure and the rings are created by boron implantation through openings in an oxide mask. Subsequently, high temperature diffusion is performed to obtain the desired p-n structure. We have built detectors with a ring structure around the main junction with different doping concentration and widths. The front window of the APD has an SiO_2 antireflective coating optimized for ~ 500 nm, and the active area of the APD is 3 mm diameter but the junction has a diameter of 5 mm. Because the time response and the capacitance depend on the junction diameter and width, and not on the active area, we have measured both parameters to show the fast response of this design. The maximum width of the depletion layer, is determined by the resistivity of the n region, and for our design it reaches approximately 140 μm. The capacitance of the APD[7] is approximately proportional to the inverse of the depletion width $C(V) \sim C_0/W$, where C_0 is a constant and W is the depletion width. This relationship allows an analytical determination of the capacitance as a function of bias voltage. It also allows a comparison between theory and experiment. The depletion layer width for a diode with a deep junction can be obtained by solving numerically the Poisson equation in one dimension[7,4]. The p-type diffusion for this type of avalanche photodiode is performed in a sealed tube under “limited source” conditions. Therefore the charge density profile obtained is characterized by the Gaussian function[7]. The solution of the Poisson equation gives the electric field distribution inside the semiconductor. The extent of the electric field gives the depletion width[7]. An important feature is that the region where the electric field is high is very extended, and not peaked as in reach-through avalanche diodes[8]. This shape provides high gain with low multiplication noise. Knowing the depletion region width, the calculated capacitance can be fitted to the experimental data, and the constant C_0 can be found. From these equations, it is also possible to calculate the gain and voltage breakdown[4]. The results show a maximum gain of approximately 500 at 1600 V. However, these voltages could not be reached because surface breakdown occurred at 1340 V. Therefore all measurements were taken with bias of 1300 V or lower. Figure 1 shows the measured (filled circles) and calculated (solid line) capacitance as a function of bias. The agreement between both lines indicates that the model is correct. At 1300 V the APD capacitance reaches approximately 20 pF, which is similar to other deep diffused APDs[5]. Because there is no saturation of the capacitance at this voltage, the device is not fully depleted. Therefore, in future devices, when the early breakdown problem is solved, and higher voltages can be applied, even lower capacitances can be achieved. Another indication of the low capacitance is the response time. For this test, the APD was illuminated with 650 nm laser connected to a fast pulser. The rise and fall time was measured with a 400 MHz oscilloscope, with the APD connected to ground through a 50 Ω resistance. The response time is shown in figure 2. The rise time is 8.5 ns and the fall time 10.6 ns.

III. Noise Characteristics

The noise from a detection system containing an APD has several sources: parallel and series noise, statistical noise and gain non-uniformity noise [9, 10]:

a) Parallel noise comes from the dark current of the APD [11] (bulk, I_b and surface, I_s), thermal noise from the feedback resistance, R_f and shot noise from the preamplifier. Parallel noise is proportional to the integration time of the preamplifier τ, and it is expressed as ENC:

$$ENC_p^2 = \frac{1}{8a_1^{'2}q^2}\left(2qI_bF + \frac{2qI_s}{M^2} + \frac{4k_BT}{M^2R_f} + \frac{2qI_g}{M^2}\right)\tau\,, \tag{1}$$

where F is the excess noise factor, I_g is the preamplifier gate current, q is the electron charge and M is the gain. The term $a_1^{'2}$ is added to account for the transit time of the holes in the depletion layer, τ_h:

$$\frac{1}{a_1^{'}} = e + \frac{\tau_h}{\tau} \tag{2}$$

where τ is the time response of the preamplifier [12], and e = 2.718.

b) The series noise stems from the capacitance of the APD, C$_d$ and preamplifier front end noise, e_n:

$$ENC_s^2 = \frac{1}{8a_1'^2 q^2}\left(4k_B T R_s C_d^2 + e_n^2 C_T^2\right)\frac{1}{M^2\tau} \tag{3}$$

where R_s is the series resistance of the APD, C_T is the APD plus preamplifier capacitance. Another series noise term which is inversely proportional to the frequency (1/f noise) has not been considered here because is it generally much smaller [13].

c) The statistical limits to the resolution in an APD are given by:

$$\sigma_{st}^2 = \mathrm{var}(n) + n(F-1) \tag{4}$$

where the excess noise factor F, accounts for the broadening of the signal due to the gain. For a light signal, such as one coming from a LED or a scintillator, we can assume that the distribution is Gaussian, and the variance is:

$$\mathrm{var}(n) = n$$

Because the illumination is uniform, differences in local gain due to non-uniformity of the structure are averaged. Also, there are no changes in local gain due to different number of electrons generated in different areas. That is, there is no change in the local electric field due to the charge density. If the gain is uniform, the statistical contribution to the energy resolution is then:

$$\sigma_{st}^2 = nF \tag{5}$$

From eq. (1), (2) and (5), we can obtain the energy resolution at the input of the preamplifier.

$$\Delta E^2 = (2.36\varepsilon)^2(\sigma_{st}^2 + ENC^2) = (2.36\varepsilon)^2(nF + ENC^2) \qquad (6)$$

where ε is the energy required to generate an e-h pair in Si (ε = 3.6 eV). From eq. (6) we can obtain the excess noise factor from the measured resolution data.

With the 3 mm diameter planar APD, have measured x-rays from a ^{109}Cd source (decay from Ag K_α = 22.16 keV) together with a pulse from a red LED.   An electronic pulse was fed directly into the preamplifier through a 0.5 pF capacitor to measure the ENC. We used standard nuclear spectroscopy electronics, that is, the APD was connected to an eV-5092 preamplifier from eV Products, a shaping amplifier 2010 from Canberra and a PC based ADC/MCA from Oxford. The LED was driven with a 74LS123 IC chip that generated a 40 ns wide pulse. The IC was triggered with a function generator. This arrangement was used because the generator can not give short square pulses at very low frequency (≈ 80 Hz). Also the duration of the light pulse has to be shorter or at least similar to the rise time of the preamplifier in order for its output pulse to be similar in shape to the x ray signal. Short pulses also allow to use short shaping times in the amplifier. Figure 3 shows the energy spectra from the ^{109}Cd source for a shaping time of 0.25 μs and a gain of 6. We have used the K_α x-ray peak (22.16 keV) from Ag and the 59.5 keV gamma ray from an ^{241}Am source to calibrate the energy of the LED and electronic pulse. The width of the electronic pulse gives us the ENC, and the width of the LED gives us the total noise in eq. (6).

The resolution (measured in keV) of the x-rays, LED, and electronic pulse is shown in figure 4 as a function of gain. The LED pulse had an equivalent energy of 42 keV, (calibrated with the x-ray signal). The electronic pulse was calibrated for each gain with the LED pulse. It can be seen that the resolution of the LED and electronic pulse are very similar, so the F parameter obtained from these curves has large errors. The intrinsic noise of the APD/preamplifier combination (second term of eq. (6)) determines the energy resolution of the electronic pulse. The signal noise (including the statistics due to the number of carriers generated and the excess noise factor) plus the intrinsic noise determine the resolution of the LED pulse. The resolution of the x-ray peak includes all previous noises. The gain non-uniformity leads to a broadening and the Fano factor leads to a narrowing of the resolution. The peak from the x-ray source cannot be seen below a gain of 3.

Figure 5 shows the F parameter determined from eq. (6) and the experimental data. Because F is a subtraction of two quantities that are very similar (see figure 4), it is very sensitive to small changes in the resolution, therefore, all resolution measurements were repeated three times to increase the accuracy. As seen in figure 5, the F parameter is lower than 2 for all gains, and increases slowly. The figure shows that the F parameter has a dependence with gain similar to other deep diffused APDs [5] which means that the performance of the planar structure is as good as other available APDs.

To show the influence of the sources of noise described in equation (1) and (3), we have plotted in figure 6, the intrinsic noise (contribution of the preamplifier-APD system) and the different components that contribute to it. In the calculation, we have used the F parameter obtained experimentally (figure 5). The values used for the different variables are taken from [4]. The measured capacitance of the APD was 50 pF. Values for the preamplifier constants are from [11]. From the figure, it can be seen that the dominant contribution comes from the preamplifier voltage noise because all measurements are taken at low gain. The preamplifier noise also is dominant when measuring photodiodes with no gain [13]. For most commercial APDs with higher gain, the dominant source of noise arises from the bulk dark current, which does not decrease with gain (figure 6, dotted line). In our measurement, the bulk and surface dark current do not play a dominant role. The experimental data, as measured with the electronic pulse, is also shown in figure 6 (open squares), it can be seen that the calculated noise agrees quite well with the experimental data.

The resolution described in eq. (6) is modified for x-ray pulses because of the additional broadening due to non-uniformity of the gain and the Fano factor. The Fano factor takes into account the fact that the processes that generate e-h pairs from x-rays in Si are not independent, because they arise from a cascade process. Therefore, the total number of electrons generated cannot be described by simple Poisson statistics. The Fano factor in Si is of the order of 0.1 [14] and improves the statistical accuracy of the signal as compared with light pulses. The variance is then modified to $\mathrm{var}(n) = fn$, where f is the Fano factor. The statistical contribution to the noise, eq. (5) is then modified to:

$$\sigma_{stx}^2 = nf + n(F-1) \tag{7}$$

Because of the Fano factor, the energy resolution of the x-rays should be better than the resolution from a light pulse, however, as can be seen in figure 5, this is not the case. The reason arises from changes in the pulse height due to variations in gain across the area of the APD. Because the x-rays generate charge carriers that are localized in an area with a diameter of a few μm in the APD, any variation of the local gain would be observed in the output signal as a broadening of the energy resolution. The gain variations are mainly due to variations in the doping concentration of the diode. This broadening is not seen with light pulses or a scintillator because the illumination is done over a larger area. To consider this effect [15], and the Fano factor, the energy resolution in equation (6) can be modified to:

$$\Delta E_x{}^2 = (2.36\varepsilon)^2(\sigma_{stx}^2 + \sigma_{NU}^2 + ENC^2) \tag{8}$$

ΔE_x is the energy resolution (in keV) of the x ray source seen by the system, σ_{NU} is the broadening of the energy resolution due to the non uniformity of the gain. Note that in reference [15], σ_{NU} is defined as $\sigma_{NU} = n\sigma_{MU}/M$, where n is the number of primary electrons.

The broadening due to non uniformity of the gain is given by 2.36 $\varepsilon\sigma_{NU}$, and it is plotted in figure 7. The broadening due to the statistical noise was subtracted from total broadening using eq. (7). The Fano factor used was 0.1 [15], and the excess noise factor was taken from figure 5. As a reference, the statistical contribution is also plotted in figure 7. It can be seen from the figure, that both sources of noise have a small increase with the gain in this range.

IV. Gain with high intensity pulses

Another effect that modifies the energy resolution is non-uniformity of the gain due to the localized generation of large number of charge carriers in a small area of the detector. This effect depends on the structure of the detector, and it has been observed with x-rays when the gain becomes large[15]. We have investigated this effect in more detail by measuring the gain with α particles from ^{241}Am. This source generates about 1.5 x 10^6 electrons in a region only a few μm wide. To measure the gain with the α source, we connected the APD to a preamplifier, a spectroscopy amplifier and to a Multichannel analyzer. Subsequently, the centroid of the pulse-height spectrum was recorded as function of bias. To measure the gain with the light source, the APD was connected to a charge sensitive preamplifier and to an oscilloscope. Then it was illuminated with a pulsed red LED. The results are shown in figure 8. It can be seen that the gain is lower when measured with particles. At a gain of 2, the α-particle gain starts to deviate from the light gain. Deviation from the light gain curve was also seen in reference [15], where they observed lower gain from 5.9 keV x-rays starting from a gain of 100. The difference with our measurement is that the number of electrons generated from the x-ray pulse in the detector is only 1600 compared to 1.5×10^6 for α particles. Therefore, they observed deviation from linearity at higher gain than us. The most probable cause for this decrease in gain is a lowering of the electric field in the small region where the charge was generated, thus the gain is lower.

We also measured the gain with a high intensity laser pulse (650 nm, 100 ns wide). The laser pulse was calibrated with a ^{241}Am source to obtain the number of electrons. The gain was measured with pulses containing ≈ 450.000 electrons each and a spot diameter of 2.5 mm and 0.3 mm, but observed no difference in the gain curves up to a gain of 6.3. Another measurement with $\approx 90 \times 10^6$ electrons per pulse did not show differences in the gain for the 0.3 mm and 2.5 mm spot size. These results indicate that the charge has to be generated in an area much smaller than 0.3 mm diameter in order to make any difference in the gain.

V. Conclusions

We have performed a detailed investigation of a new type of planar design avalanche photodiode, the data show that its performance is as good as other type of APDs, with the advantage that its built using only standard silicon processing. The capacitance was close to 20 pF at 1300 V, and the rise time at this voltage was 8.5 ns which is compatible with the low capacitance. The F parameter for gain lower than 6.3 was found to be 1.8, indicating that the APD has potential for low noise performance. The dominant contribution to the broadening of the energy resolution comes from preamplifier voltage noise, because the device is run at low gain. We also looked at the gain as measured with different sources, and found that when a large amount of charge is deposited in a small area (a few µm diameter), the gain decreases with respect to a measurement with low charge density. However, when a large amount of charge is generated in an area larger than 0.3 µm diameter, there is no change in gain. Thus for most light applications there should be no effect.

Acknowledgment

This work was supported by Fondecyt, under contract # 1990293.

References

[1] Y. Shao, R. W. Silverman, R. Farrel *et al.*, “’Design Studies of a High Resolution PET Detector Using APD arrays”, IEEE Trans. Nucl. Sci. NS-47, (2000), pp. 1051-1057.

[2]T. A. Louis, G. Ripamonte and A. Lacaita, "Photoluminescence lifetime microscopy spectrometer based on time-correlated single-photon counting with an avalanche diode detector," Rev. Sci. Inst. **61**, 11 (1990).

[3] F. Zappa, A. L. Lacaita, S. D. Cova and P. Lovati, "Solid-state single-photon detectors", Opt. Eng. **35(4)**, 938 (1996)

[4] E. Gramsch, R. E. Avila, and J. Ferrer, " Development of a novel planar construction avalanche photodiode" IEEE Trans. Nucl. Sci. Vol 48, No 4, 2001.

[5] M. Szawlowski, S. Zhang, A. DeCecco, M. Maden, M. Lindberg and E. Gramsch, " Performance of a large area avalanche photodiode" , IEEE NS Conference record, page 239, October 25 - 31, 1992, Orlando, Florida.

[6] R. Farrell, K. Vanderpuye, G. Entine and M. R. Squillante, "High resolution, low energy avalanche photodiode x-ray detectors", IEEE Trans. Nucl. Sci. **38**, No 2, pp 144-147, 1991

[7] S. M. Sze, “Physics of Semiconductor Devices”, 2nd Edition, Wiley Interscience, 1981.

[8] H. W. Ruegg, “An Optimized avalanche photodiode”, IEEE Trans. Elec. Dev. **ED-14**, 239 (1966).

[9] V. Radeka, IEEE Trans. Nucl. Sci. **2** ,51 (1974)

[10] R. Lecomte, C. Pepin, D. Rouleau, H. Dautet, R.J. McIntyre, D. McSween and P. Webb "Radiation detection measurements with a new Buried Junction silicon avalanche photodiode" Nucl. Inst. and Met. **A 423**, 92 - 102, (1999).

[11] E. Gramsch and R. E. Avila, "UV and blue-enhanced avalanche photodiodes for nuclear spectroscopy applications", Nucl. Inst. and Met. **A 414**, 299 - 306, (1998).

[12] C. A. Petrillo, R. J. McIntyre, R. Lecomte, G. Lamoureux and D. Schmitt, "Scintillation detection with large-area reach-through avalanche photodiodes", IEEE Trans. Nucl. Science **31**, 417 (1984).

[13] E. Gramsch, K.G. Lynn, M. Weber, B. DeChillo and J.R McWilliams, "Silicon PIN photodiodes in high resolution nuclear spectroscopy", Nucl. Inst. and Meth. **A311**, 529 - 538, (1992).

[14] G. F. Knoll, "Radiation Detection and Measurement", 2th edition, John Willey & Sons, New York, 1989.

[15] M. Moszynski, M. Szawlowski, M. Kapusta, M. Balcerzyk and D. Wolski, “Large Area Avalanche Photodiodes in X-Rays and Light Detection”, IEEE Trans. Nucl. Science **47**, 1297 - 1302 (2000).

Figure Captions

Figure 1. Measured capacitance of the planar-structure APD versus bias (dots) and the calculated capacitance (solid line).

Figure 2. Rise time of the planar process APD (top curve), for a 50 Ω load, illuminated with a 650 nm laser. The lower curve shows the pulser signal.

Figure 3. Energy spectra from a ^{109}Cd source, an electronic pulse and a LED, for the 3 mm diameter planar APD. The shaping time used was 0.25 μs with a gain of 6.

Figure 4. Excess noise factor versus gain for the 3 mm diameter planar-structure APD.

Figure 5. Energy resolution of the x ray, light and electronic pulse versus gain, for a 0.25 μs shaping time. The lines are a guide to the eye.

Figure 6. The energy resolution in keV of the electronic pulse (open squares) along with the components of the intrinsic noise from eq. (1) and (3). It can be seen that at these low gains, the dominant term is the preamplifier voltage noise ($e_n^2C_T^2$).

Figure 7. Contribution to the energy resolution from non uniformity of the gain and statistical noise. Variations in gain are mainly due to doping in-homogeneities.

Figure 8. Gain versus voltage measured with a LED pulse and with alpha particles from ^{241}Am.

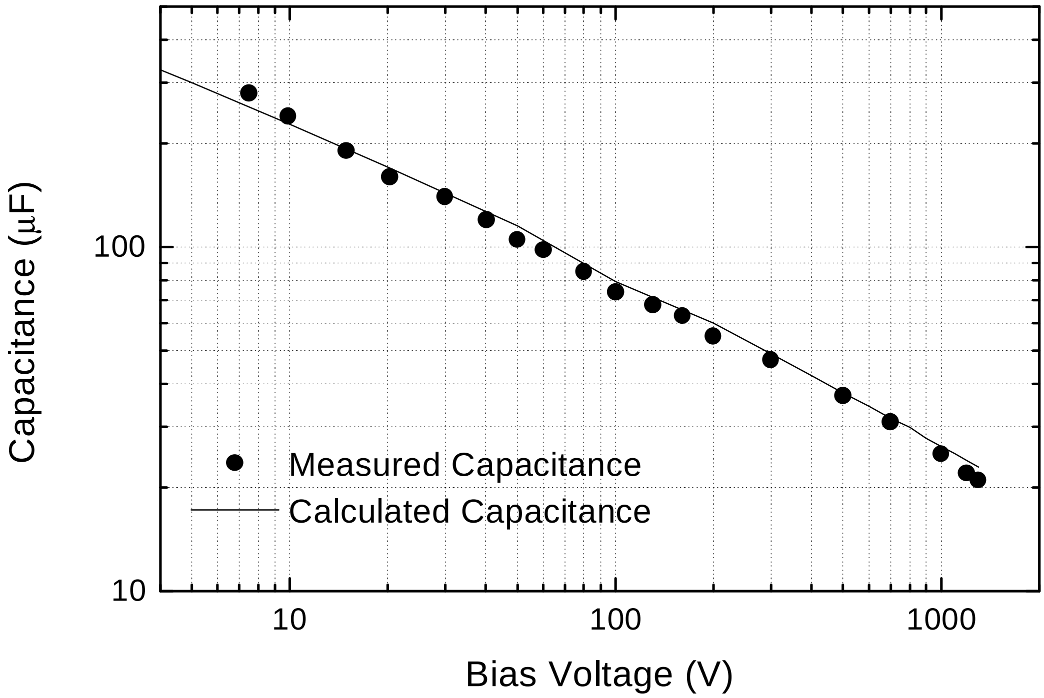
Capacitance (μF)
100
10
10
100
1000
Bias Voltage (V)
● Measured Capacitance
Calculated Capacitance

Figure 1.

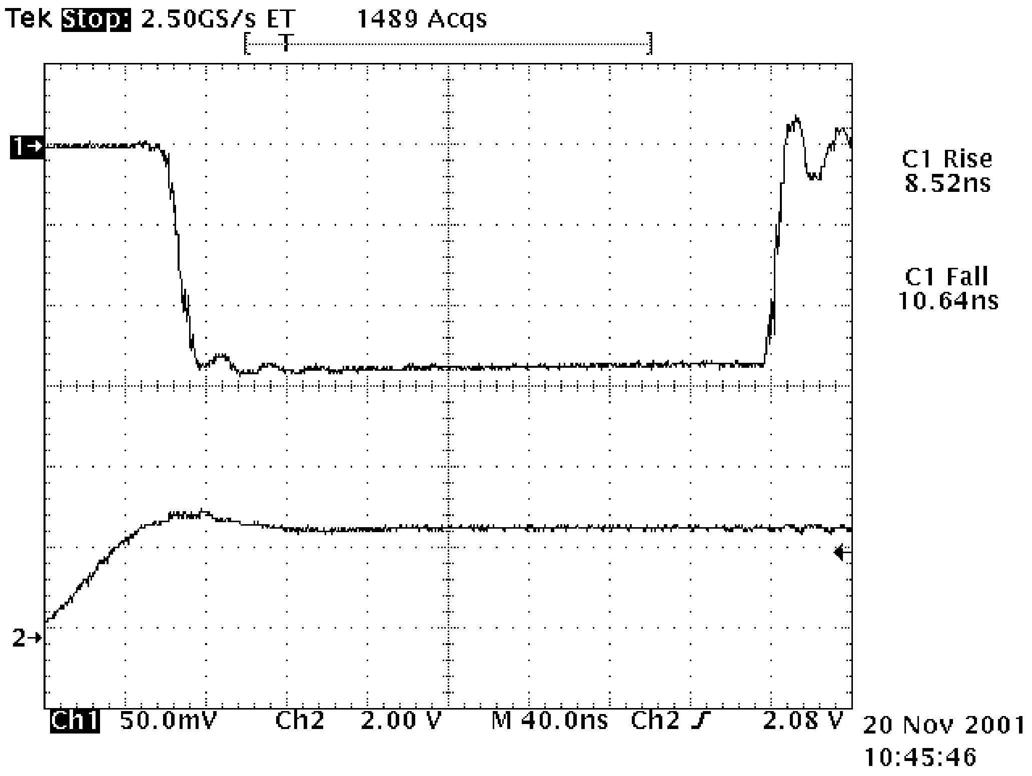
Tek Stop: 2.50GS/s ET 1489 Acqs
1→
2→
C1 Rise
8.52ns
C1 Fall
10.64ns
Ch1 50.0mV Ch2 2.00 V M 40.0ns Ch2 ƒ 2.08 V
20 Nov 2001
10:45:46

Figure 2

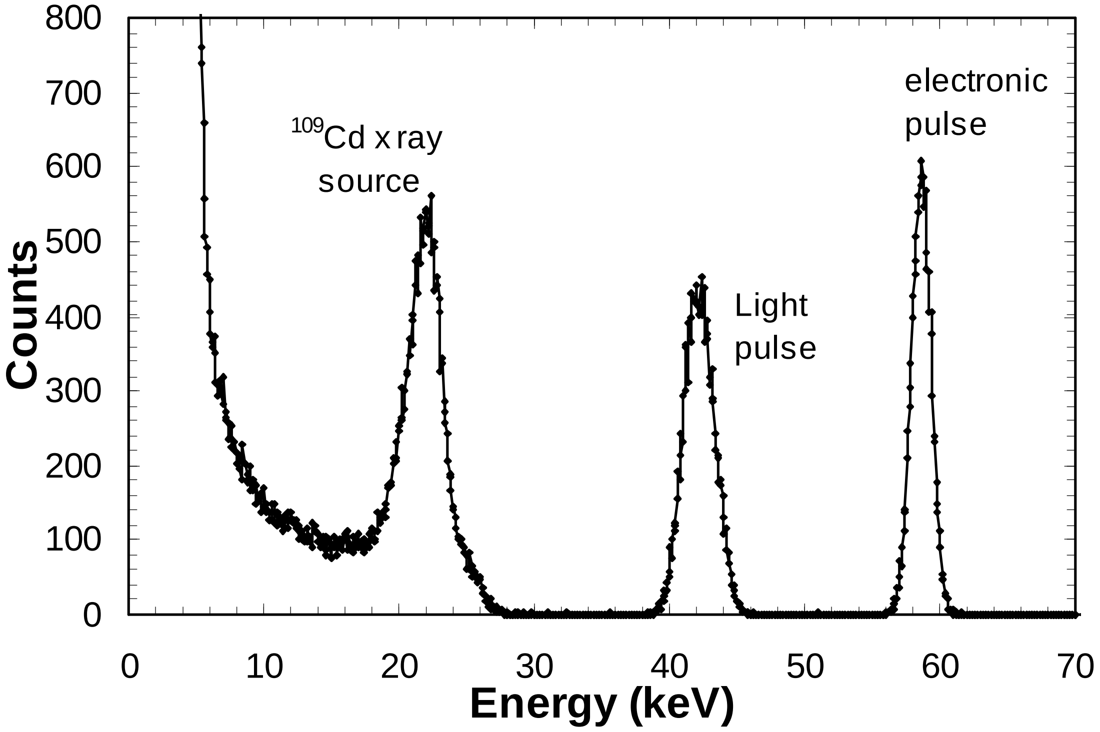
800
700
600
500
400
300
200
100
0
Counts
0
10
20
30
40
50
60
70
Energy (keV)
^{109}Cd x ray source
Light pulse
electronic pulse

Figure 3

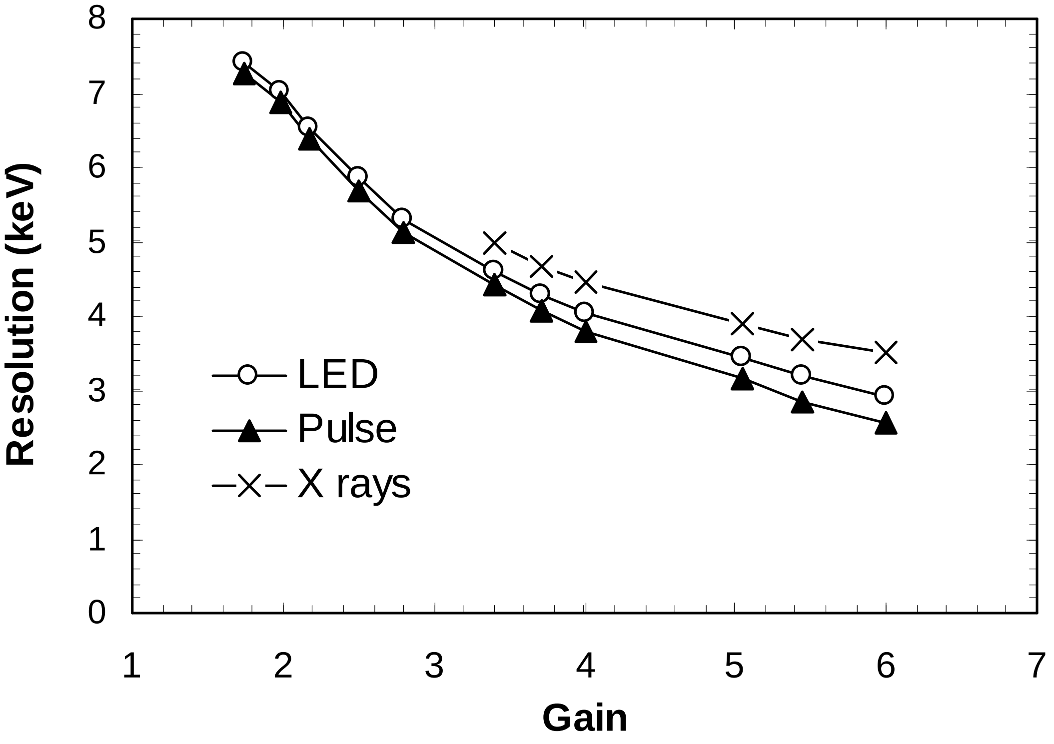

Figure 4

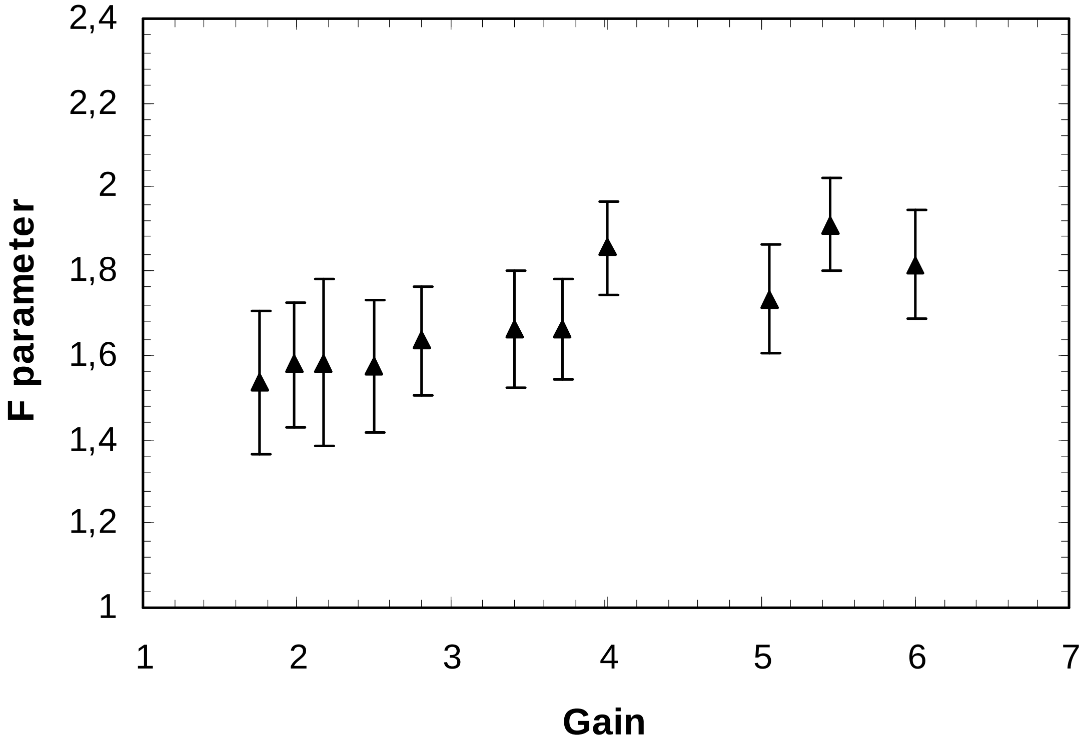

Figure 5

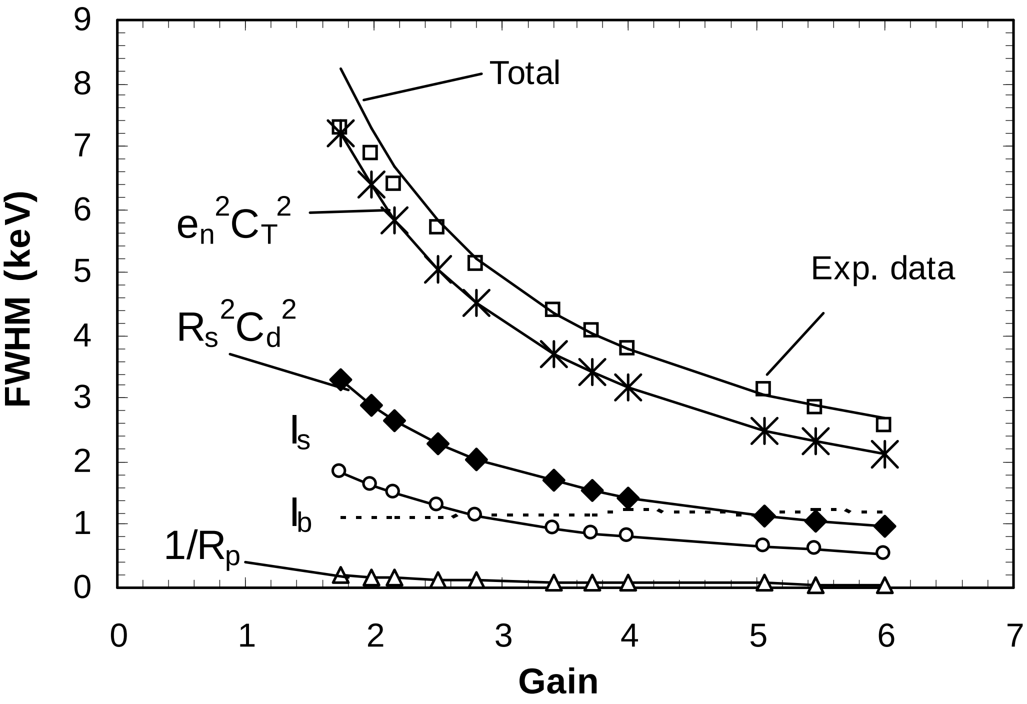

FWHM (keV)
Gain
0
1
2
3
4
5
6
7
8
9
0
1
2
3
4
5
6
7
Total
$e_n^2C_T^2$
$R_s^2C_d^2$
Exp. data
I_s
I_b
$1/R_p$

Figure 6

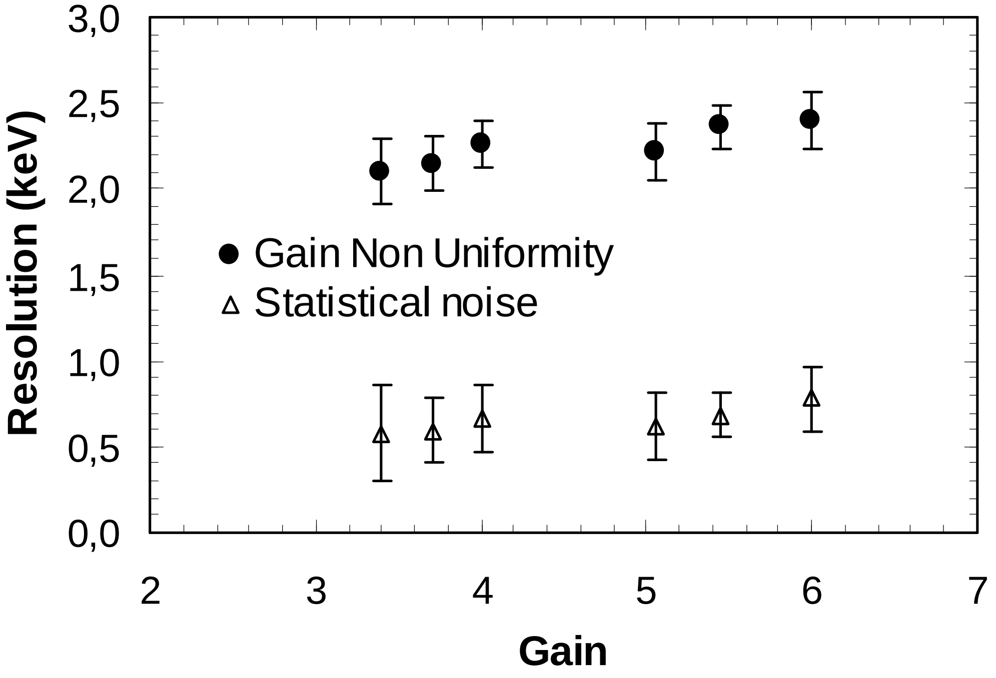
3,0
2,5
2,0
1,5
1,0
0,5
0,0
Resolution (keV)
2
3
4
5
6
7
Gain
● Gain Non Uniformity
△ Statistical noise

Figure 7

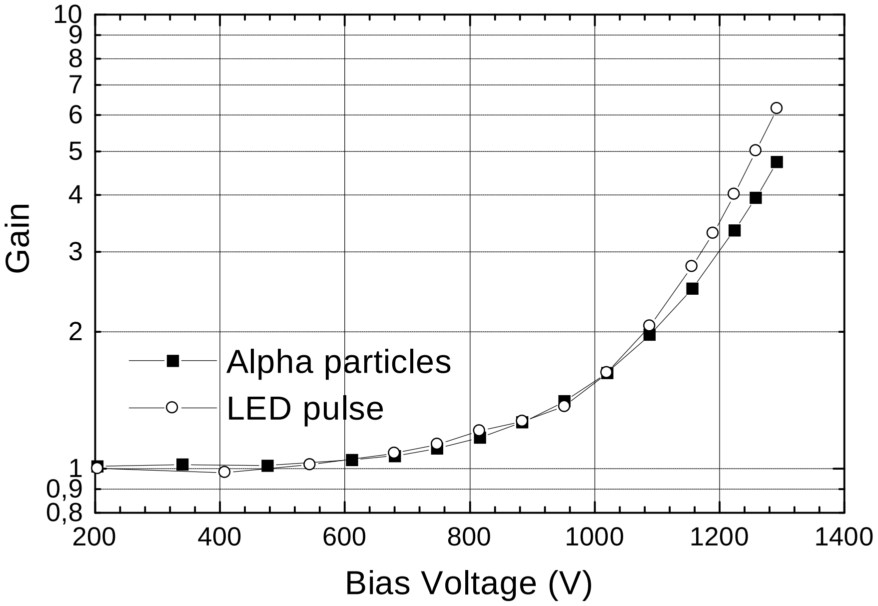
Gain
10
9
8
7
6
5
4
3
2
1
0,9
0,8
200
400
600
800
1000
1200
1400
Bias Voltage (V)
Alpha particles
LED pulse

Figure 8